Acta Astronautica 116 (2015) 166–174

Contents lists available at ScienceDirect

Acta Astronautica

journal homepage: www.elsevier.com/locate/actaastro

Second generation EmDrive propulsion applied to SSTO launcher and interstellar probe ☆

Roger Shawyer

SPR Ltd, United Kingdom

ARTICLE INFO

Article history:
Received 17 October 2014
Received in revised form
13 May 2015
Accepted 1 July 2015
Available online 10 July 2015

Keywords:
EmDrive
Propulsion
Launcher
Interstellar

ABSTRACT

In an IAC13 paper the dynamic operation of a second generation superconducting EmDrive thruster was described. A mathematical model was developed and, in this paper, that model is used to extend the performance envelope of the technology. Three engine designs are evaluated. One is used as a lift engine for a launch vehicle, another as an orbital engine for the launcher and a third as the main engine for an interstellar probe.

The engines are based on YBCO superconducting cavities, and performance is predicted on the basis of the test data obtained in earlier experimental programmes. The *Q* values range from 8×10^7 to 2×10^8 and provide high values of specific force over a range of accelerations from 0.4 m/s/s to 6 m/s/s.

The launch vehicle is an "all-electric" single stage to orbit (SSTO) spaceplane, using a 900 MHz, eight cavities, fully gimballed lift engine. A 1.5 GHz fixed orbital engine provides the horizontal velocity component. Both engines use total loss liquid hydrogen cooling. Electrical power is provided by fuel cells, fed with gaseous hydrogen from the cooling system and liquid oxygen. A 2 ton payload, externally mounted, can be flown to Low Earth Orbit in a time of 27 min. The total launch mass is 10 ton, with an airframe styled on the X37B, which allows aerobraking and a glide approach and landing.

The full potential of EmDrive propulsion for deep space missions is illustrated by the performance of the interstellar probe. A multi-cavity, fixed 500 MHz engine is cooled by a closed cycle liquid nitrogen system. The refrigeration is carried out in a two stage reverse Brayton Cycle. Electrical power is provided by a 200 kWe nuclear generator. The 9 ton spacecraft, which includes a 1 ton science payload, will achieve a terminal velocity of 0.67*c*, (where *c* is the speed of light), and cover a distance of 4 light years, over the 10 year propulsion period.

The work reported in this paper has resulted in design studies for two Demonstrator spacecrafts. The launcher will demonstrate the long-sought-for, low cost access to space, and also meet the mission requirements of the proposed DARPA XS-1 Spaceplane. The probe will enable the dream of an interstellar mission to be achieved within the next 20 years.

Abbreviations: YBCO, Yttrium Barium Copper Oxide; Q, Quality factor of a resonant circuit; kWe, Kilowatt electrical; NWPU, North Western Polytechnical University; SPR, Satellite Propulsion Research Ltd; TAA, Technology Assistance Agreement; MOD, Ministry of Defence; DARPA, Defence Advanced Research Projects Agency; USAF, United States Air Force; NSSO, National Security Space Office; NASA, National Aeronautics and Space Agency; CANNAE LLC, US private Company; GEO, Geostationary Orbit; EM, Electromagnetic; CoG, Centre of Gravity; C Band, Microwave frequency Band C; LH2, Liquid Hydrogen; LOX, Liquid Oxygen; TWTA, Travelling Wave Tube Amplifier; K, Kelvin.

☆ This paper was presented during the 65th IAC in Toronto.

E-mail address: sprltd@emdrive.com

http://dx.doi.org/10.1016/j.actaastro.2015.07.002
0094-5765/

1. Introduction

Theoretical and experimental work in the UK, China and the US has confirmed the basic principles of producing thrust from an asymmetric resonant microwave cavity. Work in the UK has progressed from deriving the basic thrust equations based on conservation of momentum and conservation of energy, to testing a Demonstrator EmDrive Engine on both static and dynamic test rigs [1].

Much of this first generation EmDrive work has been reproduced in China by a group under the direction of Professor Yang Juan at NWPU. This work has been reported in a number of peer reviewed papers. Their experimental results, first reported in 2010, give a maximum force of 720 mN for an input microwave power of 2.5 kW. The force was measured on a pendulum test rig and the direction confirmed that it was the reaction force being measured, rather than the net force due to the difference in reflection forces at each end plate [2]. This is further confirmation that EmDrive is operating as a Newtonian machine, with a thrust generated in one direction and a reaction force in the opposite direction. The acceleration measured on the SPR Demonstrator engine was in the reaction force direction, which was opposite to the thrust initially measured on the static composite balance test rig. Subsequent tests at SPR showed that both thrust and reaction force could be measured on the composite balance rig, by selection of different spring constants.

In 2009 an EmDrive technology transfer contract with Boeing was agreed. This included transfer of a flight thruster design, and was carried out under a State Department TAA and a UK export licence, approved by the UK MOD. The appropriate US government agencies including DARPA, USAF and NSSO were aware of the contract. No further details of any subsequent programme have been released into the public domain.

However, in a recent paper NASA has reported on tests of two asymmetric resonant microwave cavities [3].The NASA tapered thruster and the CANNAE thruster both work because they have a dielectric element at one end of the resonant structure. This ensures that the propagation velocity at the dielectric end is lower than at the non-dielectric end, thus giving rise to the different forces at the end plates and hence the resultant thrust. Cannae LLC is reported to be developing a superconducting version of their thruster [4].

The principle of employing a dielectric section to slow propagation at one end of the resonant cavity was first described in patent GB2229865, granted on 5 May 1993 [6] The principle was further established in patent GB2334761, granted on 19 April 2000 [7]. Note that the Patent Authorities will not grant a patent unless they are completely satisfied that the patent complies with the fundamental laws of Physics.

Later first generation cavities, developed by SPR and copied at NWPU, discarded the dielectric section due to the reduced Q values caused by dielectric losses.

Table 1 summarises the published force measurements for asymmetric resonant microwave cavities, of the EmDrive type. The results are given in ascending value of Specific force.

EmDrive type thrusters exhibit both thrust and reaction forces which are in opposite directions and can be measured using different test apparatus. Therefore they obey Newton's laws and comply with the principle of the conservation of momentum.

Fig. 1 shows that increased cavity Q gives increased specific force. Removing the dielectric section from the SPR tapered thrusters, hence increasing Q by decreasing losses, gave a clear increase of specific force. The CANNAE tests show that for the same configuration, changing from a copper device at room temperature, to a superconducting Niobium device cooled with liquid Helium with a Q of 1.08×10^7 gave an increase of specific force by a factor of 550.

Having completed all the basic R&D on first generation EmDrive at SPR, work was then carried out on second generation, superconducting technology. The aim was to increase the first generation specific force of 300 mN/kW to a target of 10 kN/kW. These thrust levels will require extremely high Q values for the resonant cavity, and although such values are regularly obtained in particle accelerators, their performance under acceleration had not been investigated. The operation of such thrusters was modelled mathematically, and a severe reduction in thrust under acceleration was predicted, due to the internal Doppler shifts in the cavity. In a typical result, the reduction to 1% of maximum static thrust was calculated for a Doppler shift of 2.3 Hz, at an operating frequency of 1.3 GHz. This was predicted for a cavity Q of 5.6×10^8 at an acceleration of 0.005 m/s/s. Compensation techniques were investigated and an early design study was made for a GEO launch vehicle. [8].

The work described in this paper is a continuation of the EmDrive dynamic modelling, to extend the performance envelope over three engine designs and two Demonstrator spacecraft.

Table 1
Summary of published Specific forces.

Thruster design	Specific force mN/kW	Force direction	Reference
CANNAE room temperature	1.73	Thrust	[3]
NASA tapered cavity with dielectric section	6.86	Thrust	[3]
SPR tapered cavity with dielectric section	18.8	Thrust	[1]
SPR	214	Thrust	[1]
Demonstrator engine	243	Reaction	
NWPU thruster	288	Reaction	[2]
SPR flight thruster	330	Reaction	[5]
CANNAE superconducting	952	Thrust	[4]

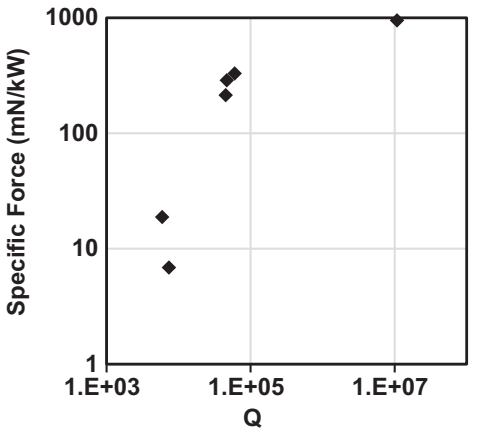

Fig. 1. Published Q and specific force data from [1–5].

2. Dynamic model

Although the world wide experimental work described has clearly validated the static thrust mechanism of an asymmetric resonant microwave cavity, no experimental verification of the conservation of energy for an accelerating EmDrive thruster has yet been published. The simple theoretical view is that acceleration of the cavity causes a reduction in stored energy, a consequent reduction in the loaded Q value, and thus a reduction in thrust.

A detailed mechanism was described and modelled in [8]. In summary as an EM wave cycle progresses through its multiple reflections in the resonant cavity, the acceleration causes Doppler shifts at each end plate. Because the guide velocity is different at each end, the Doppler shifts are different, even for a constant rate of acceleration. This build-up of net frequency shift causes a widening of the spectrum of the standing wave pattern, and causes much of the power spectrum to fall outside the narrow bandwidth of the resonant cavity. Clearly this effect will increase with increasing cavity Q, as the number of reflections increase, together with the reduction in bandwidth. The effect on specific force approximates to a square law when Q is the variable. Therefore with the increase in Q of up to 5 orders of magnitude from a first generation to a second generation engine, the effects of acceleration will change dramatically.

The mathematical model showed that for a first generation EmDrive engine, with a Q of 5×10^4 the effect is negligible for typical in-orbit propulsion applications. However, for a second generation with a Q of 3.9×10^7 the specific force of 173 N/kW is reduced to 11 N/kW for an acceleration of 20 m/s/s. To achieve the target specific force of 10 kN/kW a number of compensation techniques were investigated.

3. Design considerations

A fundamental problem with any asymmetric resonant cavity is the need to minimise phase distortion across the wavefront, due to path length variation. As the theoretical Q of the cavity increases, the actual Q achieved becomes more dependent on the geometry and machining tolerance of the cavity.

A number of different geometries have been investigated at SPR Ltd, but the simplest configuration is illustrated in Fig. 2.

The cavity comprises a small convex end plate, a truncated conical side wall section, and a large concave end plate. The end plate radii R1 and R2 are selected such that $R2-R1=L1$ where L1 is the length of the side wall. This geometry ensures that the EM wavefront propagates between the end plates with every point on the wavefront travelling along a radius line of length L1, centred at point O. This constant path length over the wavefront ensures that phase distortion over the very large number of reflections within a high Q cavity, is minimised, and the value of Q that is achieved in practice approaches the theoretical maximum. Note that this configuration ensures that there is no orthogonal component of the guide velocity reflected from the side wall, thus ensuring a zero side wall force component in the axial plane.

Fig. 3 shows a diagram of a superconducting cavity mounted in a Dewar containing a liquefied gas coolant. The internal cavity walls are coated with a High Temperature Superconducting material such as Yttrium Barium Copper Oxide (YBCO) which is superconducting at liquid Nitrogen temperature and below.

Microwave power, typically 20 kW for a lift engine, is fed to the cavity via an input waveguide. To compensate for the decrease in frequency due to the Doppler shift under acceleration, the axial length of the cavity is increased by piezoelectric elements, mounted between the side wall and the small end plate. A change in axial length of 22×10^{-6} m was calculated for a 915 MHz cavity accelerating at 0.3 m/s/s. The voltage controlling the length of the piezoelectric element is determined by a processor, fed by the output of an accelerometer. The overall control schematic is given in Fig. 4, which shows the processor also controls the frequency and pulse length of the signal sent to the microwave power amplifier. The control inputs for these functions are outputs from the accelerometer and a detector mounted in the wall of the cavity. Further information is given in [9].

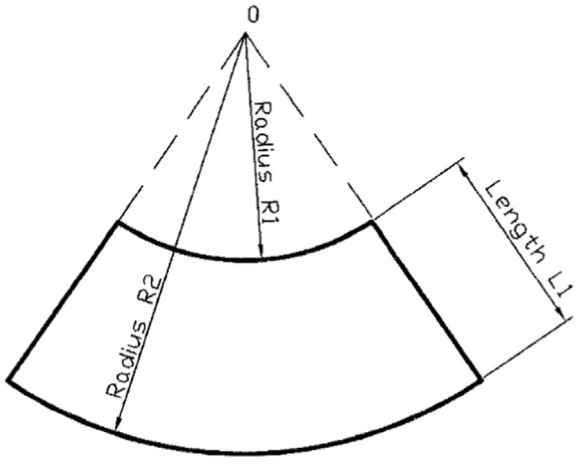

Fig. 2. Cavity geometry for spherical end plates.

Clearly, the axial length extension needs to be limited to the time taken for the initial wavefront to decay to a level where its thrust contribution is minimal. During this extension pulse period, the input frequency must be modified to optimise the portion of the input spectrum that remains within the bandwidth of the cavity. The dynamic model has been used to investigate the algorithms necessary to control frequency and pulse length to produce maximum specific force, for a range of Q values and acceleration rates.

One result of this work has been to conclude that practical second generation engines will need to consist of multiple cavities with input power switched between them, thus avoiding the need for very high peak power microwave sources. This multiple cavity concept also results in a smoothed average thrust output, thus minimising the mechanical stresses that would be imposed on a spacecraft using a single pulsed cavity.

To investigate the performance envelope of such a multi-cavity superconducting engine, two applications were studied. These were Demonstrator spacecraft with very different propulsion requirements. The first is an "all-electric" single stage to orbit (SSTO) spaceplane, capable of placing a 2 ton payload into Low Earth Orbit (LEO). The spaceplane requires two different engines, one to provide lift, the other to provide orbital velocity. The short operating time for these engines allows a total loss cooling system to be employed with liquid hydrogen being the selected coolant. Electrical power is generated by fuel cells.

The second Demonstrator is an interstellar probe capable of accelerating a 1 ton payload up to a high fraction of the speed of light over a 10 year propulsion period. These requirements result in a closed cycle liquid nitrogen cooling system and a direct cycle, nuclear reactor to provide the electrical power.

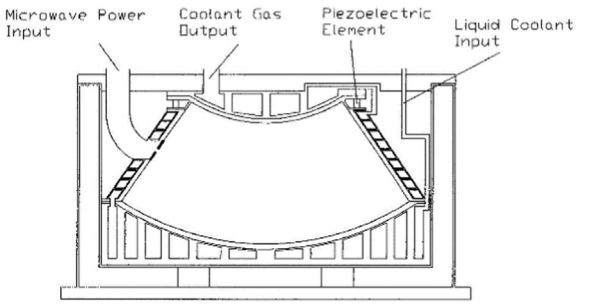

Fig. 3. Superconducting cavity, cooled by liquid gas and mounted in a Dewar.

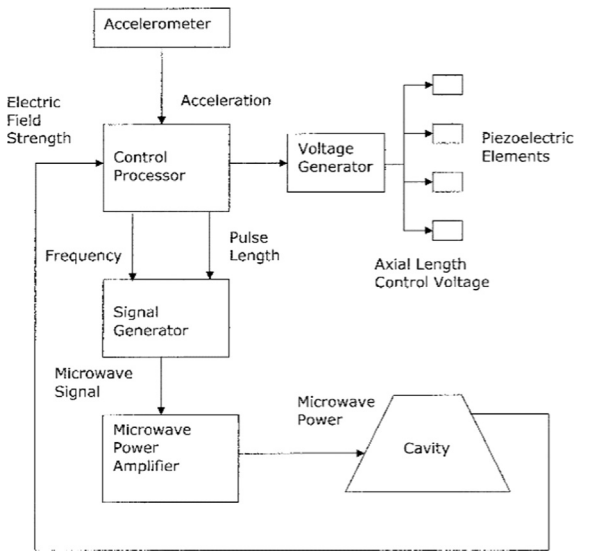

Fig. 4. Schematic of control system for Doppler compensation.

4. Engine descriptions

4.1. Spaceplane lift engine

The basic requirement of this engine is to support the total mass of the spaceplane, (a nominal 10 ton) and to provide a low acceleration flight profile to reach LEO altitude. The engine comprises eight rectangular kovar cavities, internally coated with YBCO, cooled with liquid hydrogen and operating at 915 MHz.

This single lift engine is mounted in a two axis gimballed spherical housing 790 mm in diameter, with the cavities in a 4×2 configuration as shown in Fig. 5. The rectangular cavities are mounted in blocks of four, with one block mounted vertically on top of the other.

Input power is switched between the eight cavities over a 220 ms cycle with the power pulsed for one eighth of the cycle, but with the extension being applied non linearly throughout the cycle as shown in Fig. 6. The total thrust is therefore the sum of eight of the single cavity thrust characteristics shown in Fig. 6, but staggered through the cycle.

The resulting specific force varies approximately linearly for the compensated engine over an acceleration range of 0 to 1 m/s/s with a specific force of 667 N/kW at a vertical acceleration of 0.39 m/s/s.

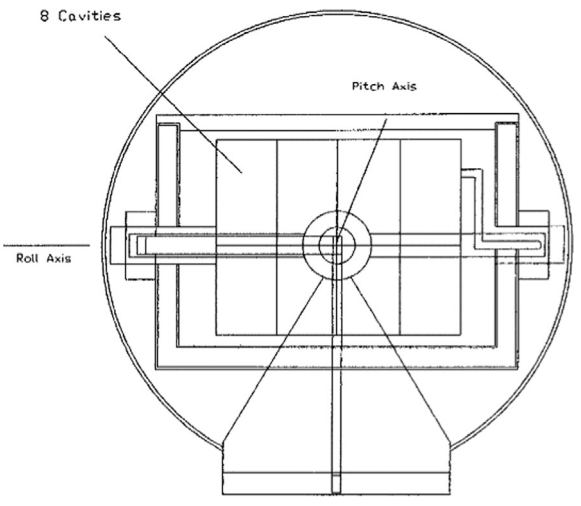

Fig. 5. Eight cavity Lift engine mounted in a two axis gimbal mechanism.

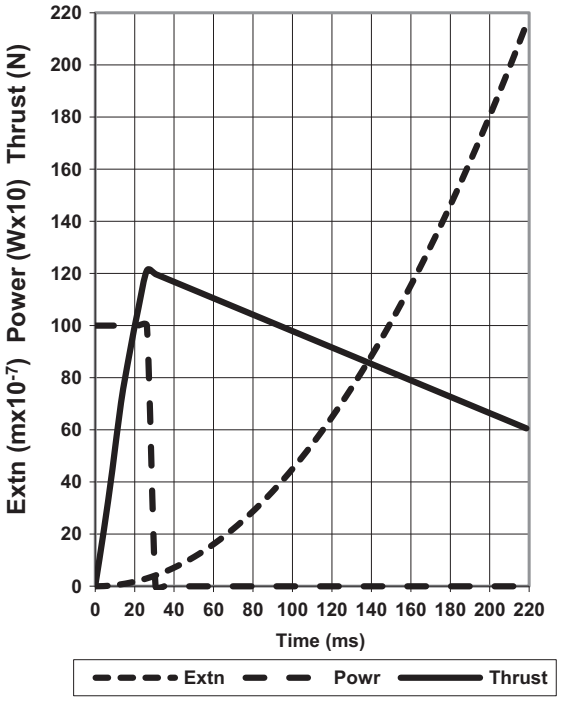

Fig. 6. Power and extension cycle applied to a single cavity, showing resultant thrust.

4.2. Spaceplane orbital engine

The basic requirement of this engine is to accelerate the spaceplane up to the orbital velocity of 7800 m/s. As with the lift engine, the design is based on eight cavities, but because a lower Q is needed to allow a greater acceleration, the operating frequency is increased to 1.5 GHz.

The orbital engine has the eight rectangular cavities stacked in a 2×4 configuration with the acceleration vector aligned with the axis of the spaceplane. The rectangular cavities are mounted in blocks of two, with each block mounted horizontally in line. The switching cycle is shorter than the lift engine, operating over a 90 ms cycle, but with similar shaped extension, power and thrust characteristics as shown in Fig. 6.

The nominal specific force for the orbital engine is 185 N/kW at an acceleration of 6 m/s/s.

4.3. Interstellar Probe Main Engine

The requirements for the Interstellar Probe Main Engine are significantly different from those of the spaceplane engines, but once again an eight cavity engine is chosen. Kovar rectangular cavities coated with YBCO are stacked in a 2×4 configuration, but this time the coolant is liquid nitrogen and the operating frequency is 500 MHz. The higher operating temperature is compensated by the lower operating frequency, to provide a nominal specific force of 304 N/kW for an acceleration of 1 m/s/s.

5. Spacecraft and mission descriptions

5.1. Spaceplane description

The requirement specification for the spaceplane was based on the original DARPA requirements for the XS-1 spaceplane, [10]. This called for the capability of delivering a 2 ton payload to LEO using a reusable Mach 10 aircraft, and an upper stage. The similarity between the requirement and early flight profiles of a Demonstrator version of the EmDrive Hybrid Spaceplane, described in [11] were noted. This led to a design study with the aim of providing a step change in the solution, namely a Single Stage to Orbit spaceplane, thus removing the need for the upper stage on XS-1 or on the earlier Hybrid Spaceplane.

The key technical challenges of the XS-1 programme were retained for our design study, namely:

- A reusable vehicle designed for aircraft-like operations.
- Robust airframe composition leveraging state-of-the-art materials, manufacturing processes, and analysis capabilities.
- Durable, low-maintenance thermal protection systems that provide protection from temperatures and heating rates ranging from orbital vacuum to atmospheric re-entry and hypersonic flight.
- Reusable, long-life, high thrust-to-weight, and affordable propulsion systems.
- Streamlined “clean-pad” operations dramatically reducing infrastructure and manpower requirements while enabling flight from a wide range of locations.

These challenges meant that the EmDrive propulsion requirements would be simplified by the adoption of aerobraking glide descent and horizontal landing. A further simplification of the study was to assume an airframe styled on the operational USAF X-37B, which has been proven over a number of missions.

An outline diagram of the SSTO spaceplane is given in Fig. 7. This shows the lift engine centrally mounted above the CoG of the vehicle, with three small, C-band 2-axis gimballed EmDrive thrusters, to give roll pitch and yaw control. The bulk of the volume is taken up with the two liquid hydrogen tanks, which provide 21,000 l (1486 kg) of LH2. The large volume of LH2 provides cooling for the EmDrive engines, at a maximum flow rate of 1.05 kg/s. A fraction of the resulting gaseous H2 is used in the fuel cells for power generation and cooling. The liquid oxygen tanks provide 260 l (296 kg) of LOX for power generation in the fuel cells only. The fuel cells are rated at a nominal 500 kW and require a maximum LOX flow rate of 0.164 kg/s.

The 2000 kg payload is mounted on rails on the top surface of the spaceplane. A launch mass of 9860 kg has been estimated, including payload, with a vehicle dry mass of 6080 kg. The mass budget is given in Table 2.

5.2. SSTO spaceplane mission

The original launch vehicle based on second generation EmDrive technology assumed EmDrive would provide the

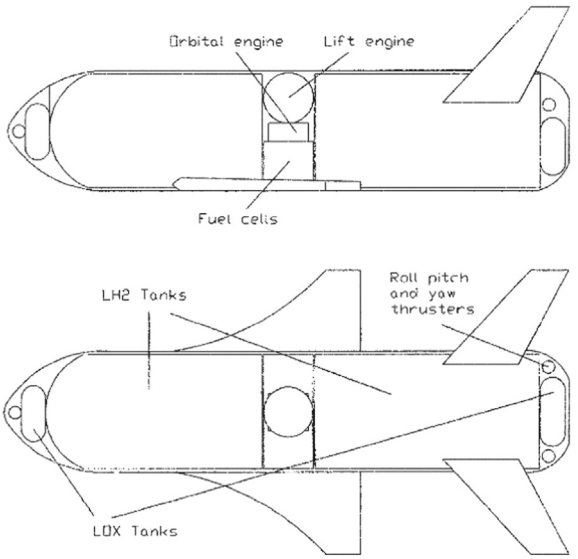

Fig. 7. Outline diagram of SSTO spaceplane.

Table 2
Spaceplane mass budget.

Item	Mass (kg)
LH2	1486
LOX	296
LH2 tanks	223
LOX tanks	44
TWTAs	1163
Fuel cells	1416
Lift engine	85
Orbital engine	55
Attitude engines	90
Airframe	3000
Payload	2000
Launch mass	9858

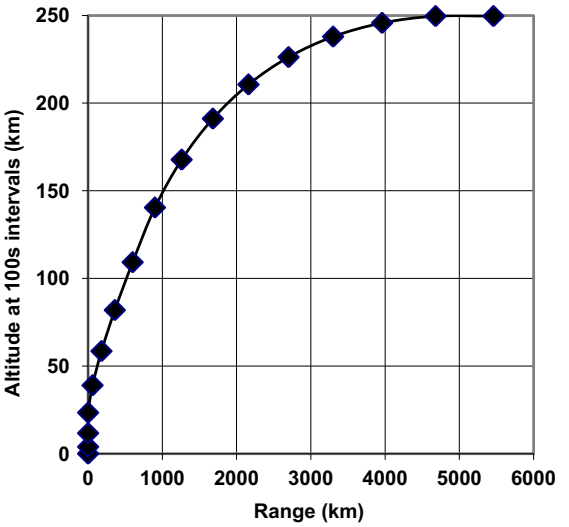

Fig. 8. Spaceplane ascent profile showing altitude at 100 s intervals versus range.

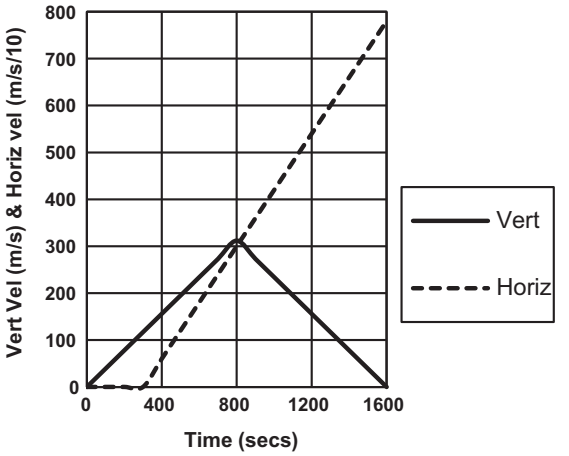

Fig. 9. Spaceplane velocity profile showing horizontal and vertical velocity components versus flight time.

lift and a conventional expendable rocket would propel the orbital module [11]. This solved the classic "return to launch site" problem by minimising the horizontal velocity of the carrier spaceplane. However the expendable orbital module remained a cost barrier.

The SSTO Spaceplane solves the return to launch site problem by orbiting the complete spaceplane and using the EmDrive lift engine to provide initial de-orbit braking, whilst aerobraking and glide landing complete the return in the same manner as the X37B spaceplane.

The spaceplane ascent range profile is illustrated in Fig. 8 with velocity profiles given in Fig. 9. In the initial 300 s, only the lift engine is operational, giving a vertical acceleration of 0.39 m/s/s to an altitude of 23 km. At this point the orbital engine is started and the spaceplane starts to fly down range with an acceleration of 6 m/s/s. After 800 s the power to the lift engine is reduced to give a constant deceleration of 0.39 m/s/s.

After 1600 s total flight time the vertical velocity component is zero with a horizontal component of 7.8 km/s corresponding to the required orbital velocity at an altitude of 250 km. Clearly the mission profile minimises g forces and aerodynamic and thermal stresses on the airframe during the ascent phase, with the result that unfaired payloads, with generous dimensions, may be attached to the top rails.

Further mission optimisation with a more advanced engine design is currently being undertaken. This will give an EmDrive controlled descent and remove the mechanical and thermal stresses of the aerobraking and glide return. The result will be a lighter, conventional, aircraft type airframe.

5.3. *Interstellar probe description*

The nominal 10 year propulsion period for the Interstellar Probe is defined by the design of the nuclear reactor and electrical generating system. This is based on the work described in [12].

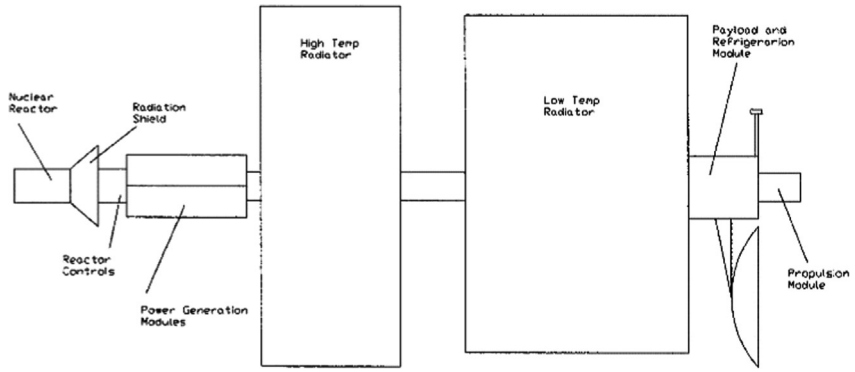

Fig. 10. Outline diagram of Interstellar probe.

Table 3
Interstellar probe mass budget.

Item	Mass (kg)
Reactor	528
Shield	600
Reactor controls	31
Heat exchangers	366
Generators	1612
High temp radiator	885
Main engine	600
Attitude engines	90
Cooling turbine	510
Low temp radiator	1314
Structure	1400
Payload	1000
Total	8936

A 1.2 MW thermally rated reactor, using a direct Brayton cycle design operating at 1300 K, will provide 200 kW of electrical power, with a high temperature radiator operating between 800 K and 505 K. This is coupled to the propulsion system by a truss structure. The propulsion system comprises the ISP main engine with its refrigeration module and a low temperature radiator operating between 280 K and 78K. The refrigeration module is a reverse Brayton cycle with 2 stage turbines.

The complete spacecraft is illustrated in Fig. 10, and has overall dimensions of 28.2 m in length and 12.8 m in width across the high temp radiator. The mass budget is given in Table 3.

5.4. High velocity operation

Clearly an interstellar mission with a terminal velocity approaching two thirds of the speed of light requires consideration of the effect of high velocity operation on EmDrive operating principles.

To investigate the effect of high velocities on the thrust of an EmDrive engine, first consider a cavity at rest.

Assume a wavefront travels a total distance of D inside the cavity, before all the energy is dissipated in wall losses, where:

$$D = 2Q_u L \tag{1}$$

where Q_u = Unloaded Q value.

L = Cavity length.

The time to travel distance D is defined as the time constant of the cavity T_c, where:

$$T_c = \frac{Q_u}{F_0} \tag{2}$$

Next, assume that at velocity V_1, the cavity travels a distance of x during the time T_c.

From a Newtonian viewpoint, during this period the wavefront would have travelled a total distance of $D+x$.

However Special Relativity theory shows that the velocity of propagation of the wavefront is independent of the velocity of the cavity, therefore the total distance travelled by the wavefront must remain constant. Thus as the cavity velocity increases, the distance travelled by the wavefront inside the cavity D must decrease. For D to decrease, Q_u must decrease.

Thus from Eq. (1), at velocity V_1:

$$D = 2Q_1 L + x$$

where:

$$Q_1 < Q_u$$

Thus

$$2Q_1 L + x = 2Q_u L \tag{3}$$

Now $x = V_1 T_c$

Therefore from Eqs. (2) and (3):

$$2Q_1 L + V_1 \frac{Q_u}{F_0} = 2Q_u L$$

Then solving for Q_1:

$$Q_1 = Q_u \left\{ 1 - \frac{V_1}{2LF_0} \right\} \tag{4}$$

5.5. Interstellar probe mission

The interstellar probe mission profile is given in Fig. 11. Although the nominal acceleration is 1 m/s/s, the velocity profile has to be modified first by the EmDrive high velocity effect described in Section 5.4, and then by the additional energy required due to relativity effects.

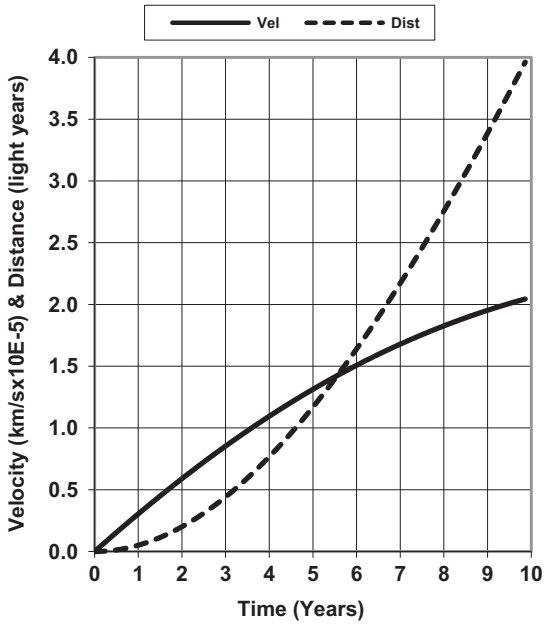

Fig. 11. Interstellar probe mission profile showing velocity and distance versus flight time.

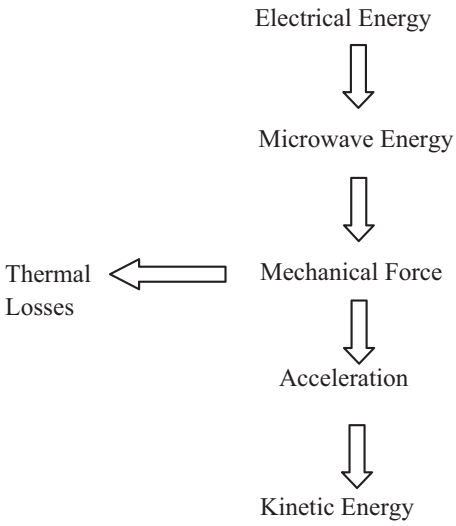

Fig. 12. Schematic of overall energy flow.

This latter factor F_R is given by

$$F_R = \frac{1}{\sqrt{1-\frac{v_1^2}{c^2}}} \tag{5}$$

where v_1 = spacecraft velocity.

Thus after 9.86 years of propulsion the velocity has reached 204,429 km/s at a distance of 3.96 light years. It is anticipated that following the propulsion period, all electrical power would be utilised by the payload communications system, during the subsequent target fly by.

6. Mission energy analysis

A useful method of reviewing the results of the two Demonstrator missions is to calculate the total energy balance of the acceleration phases of the missions. This enables the energy efficiency to be calculated in terms of the total kinetic energy of the spacecraft at terminal velocity, divided by the total energy input during the acceleration period. The overall energy flow is illustrated in Fig. 12.

In an EmDrive engine, microwave energy is converted to mechanical force according to the thrust equation, derived from the basic radiation pressure equation:

$$F = \frac{2P_0}{c} \tag{6}$$

where F = Force

P_o = Incident power

The actual thrust equation, derived in [1] is given by:

$$T = \frac{2P_0 Q_u S_0}{c}\left\{\frac{\lambda_0}{\lambda_{g1}} - \frac{\lambda_0}{\lambda_{g2}}\right\} \tag{7}$$

where

$$S_0 = \left\{1 - \frac{\lambda_0^2}{\lambda_{g1}\lambda_{g2}}\right\}^{-1}$$

This can be simplified to:

$$T = \frac{2P_0 Q_u K_d}{c} \tag{8}$$

where Q_u = Unloaded Q of cavity

$$K_d = So\left\{\frac{\lambda_0}{\lambda_{g1}} - \frac{\lambda_0}{\lambda_{g2}}\right\}$$

Kd is referred to as the Design Factor.

The instantaneous mechanical power produced by this conversion is given by:

$$P_{mech} = TV_1 \tag{9}$$

where V_1 = spacecraft velocity

Over the acceleration period, the total energy input to the spacecraft is given by:

$$E_{in} = TV_{av}.t_a \tag{10}$$

where V_{av} = average spacecraft velocity

t_a = acceleration period

Substituting Eq. (8) in Eq. (10)

$$E_{in} = \frac{2P_0 Q_u K_d V_{av} ta}{c} \tag{11}$$

The kinetic energy of the spacecraft at terminal velocity V_T is given by:

$$E_k = \frac{MV_T^2}{2} \tag{12}$$

where M = mass of spacecraft

V_T = terminal velocity

The efficiency of the EmDrive engine can therefore be calculated from:

$$e = \frac{E_k}{E_{in}} \tag{13}$$

Table 4
Spaceplane parameters.

Parameter	Value	Units
P_0	324	kW
Q	8×10^7	
K_d	0.7706	
V_T	7800	m/s
T_a	1300	s
M	8059	kg

Table 5
Interstellar probe parameters.

Parameter	Value	Units
P_0	29.6	kW
Q	1.25×10^8	
K_d	0.7725	
V_T	2.04×10^8	m/s
t_a	9.86	years
M	8936	kg

The in orbit SSTO spaceplane parameters are given in Table 4.

From Eq. (11):

$$E_{in} = 6.75 \times 10^{11} \text{J}$$

From Eq. (12)

$$E_k = 2.45 \times 10^{11} \text{ J}$$

Therefore from Eq. (13) orbital thruster efficiency

$$e_{to} = 0.363$$

For overall mission efficiency the electrical power input from the fuel cells should be used, reducing the mission efficiency to

$$e_{mo} = 0.243$$

The interstellar probe parameters are given in Table 5.

From Eq. (11)

$$E_{in} = 6.04 \times 10^{20} \text{ J}$$

From Eq. (12)

$$E_k = 1.87 \times 10^{20} \text{ J}$$

Therefore from Eq. (13) interstellar thruster efficiency

$$e_{ti} = 0.31$$

For the overall mission efficiency, the thermal rating of the nuclear reactor should be used (1.2 MW) for the power input, rather than the microwave power input (29.6 kW). This reduces the mission efficiency to

$$e_{mi} = 0.0076$$

Clearly, the two engine designs were optimised for spacecraft masses and acceleration rates, and resulted in similar thruster efficiencies. However, the extended interstellar mission time required the use of a nuclear reactor power source and a closed cycle thruster cooling system. The low thermal efficiencies of these subsystems resulted in the low interstellar mission efficiency.

7. Conclusions

The two spacecraft design studies and the three different EmDrive engine designs have illustrated the complexity introduced by the Doppler model of EmDrive acceleration. The compensation techniques described are a first attempt at reducing the loss of thrust due to accelerating a high Q cavity. New techniques are currently under investigation to optimise the engine performance whilst simplifying the design. A number of research groups worldwide are now working towards the manufacture and test of Demonstrator Thrusters.

Nevertheless, the performances offered by the SSTO Spaceplane and the Interstellar Probe are a major improvement over vehicle designs based on conventional propulsion systems. Second generation EmDrive offers the best solution for low cost access to space, and for a near term interstellar mission.

References

[1] R.J. Shawyer, Microwave propulsion – progress in the EmDrive programme SPR Ltd UK IAC-08-C4.4.7, Glasgow, 2008.
[2] Juan Yang, et al., Prediction and Experimental Measurement of the Electromagnetic Thrust Generated by Microwave Thruster System NWPU Xi'an China Chinese Physical Society and IOP Publishing Ltd., 2013.
[3] D. Brady, et al., Anomalous thrust production from an RF test device measured on a low thrust torsion pendulum. NASA US AIAA Joint Propulsion Conference, Cleveland, 2014.
[4] G.P. Fetta, Experimental and numerical results on a superconducting prototype of a new thruster technology which requires no on-board propellant to generate thrust. Cannae LLC US AIAA Joint Propulsion Conference, Cleveland, 2014.
[5] R.J. Shawyer, The EmDrive – a new satellite propulsion technology SPR Ltd UK 2nd Conference on disruptive technology in space activities, Toulouse, 2010.
[6] Patent GB2229865, Electrical Propulsion Unit for spacecraft Filed 01 November 1988, Granted 05 May, 1993.
[7] Patent GB2334761, Microwave Thruster for Spacecraft Filed 29 April 1998, Granted 19 April, 2000.
[8] R.J. Shawyer, The dynamic operation of a high Q EmDrive microwave thruster SPR Ltd UK IAC-13, C4,P, 44pl, x17254 Beijing, 2013.
[9] Patent GB2493361, High Q Microwave Radiation Thruster Filed 01 August 2011, Published 06 February, 2013.
[10] Special Notice DARPA-SN-14-01 Experimental Spaceplane (XS-1) Proposers Day 7 October, 2013.
[11] R.J. Shawyer, The EmDrive programme – implications for the future of the aerospace industry SPR Ltd UK CEAS 2009 Manchester, 2009.
[12] A. Donaldson, R. Blott, M. Mazzini, High power nuclear electric propulsion IEPC-2011-061 Wiesbaden, 2011.